

## DIFFERENCES IN DROUGHT ADAPTATION BETWEEN SUBSPECIES OF SAGEBRUSH (*ARTEMISIA TRIDENTATA*)

KIMBERLEY J. KOLB<sup>1</sup> AND JOHN S. SPERRY

Department of Biology, University of Utah, Salt Lake City, Utah 84102 USA

**Abstract.** Three subspecies of *Artemisia tridentata* occupy distinct habitats in the Great Basin of North America: ssp. *wyomingensis* in low, arid elevations; ssp. *vaseyana* in high, mesic elevations; and ssp. *tridentata* in intermediate zones. We evaluated differences in the drought experienced and drought tolerance among the subspecies. Drought tolerance was measured by two traits: the xylem pressure ( $\Psi_x$ ) causing xylem cavitation and  $\Psi_x$  causing loss of leaf turgor ( $\Psi_{\text{tip}}$ ). As expected from habitat, ssp. *wyomingensis* experienced a more severe summer drought than ssp. *vaseyana* (minimum  $\Psi_x = -7.5$  MPa and  $-3.8$  MPa, respectively). Despite the large difference in drought exposure, the subspecies exhibited similar drought responses, including a reduction in transpiration ( $E$ ) below  $0.5 \text{ mmol}\cdot\text{s}^{-1}\cdot\text{m}^{-2}$ , a shedding of 60–65% of foliage, and >95% decline in soil-to-leaf hydraulic conductance. The similarity in the drought response was consistent with pronounced differences in  $\Psi_x$ , causing 50% loss in xylem conductivity by cavitation ( $\Psi_{50}$ ). The  $\Psi_{50}$  was  $-4.9$  MPa in ssp. *wyomingensis* vs.  $-3.0$  MPa in ssp. *vaseyana*; ssp. *tridentata* was intermediate ( $\Psi_{50} = -3.9$  MPa). Differences in cavitation resistance were preserved in a common garden, suggesting that they arose by genetic differentiation. A water transport model indicated that the greater cavitation resistance in ssp. *wyomingensis* was a necessary adaptation for its more arid habitat, and that the similar restrictions of  $E$  among subspecies were required to avoid hydraulic failure. The  $\Psi_{\text{tip}}$  was also lower in ssp. *wyomingensis* than in ssp. *vaseyana*. Although  $\Psi_{\text{tip}}$  decreased in both subspecies during drought, the adjustment was not sufficient to maintain turgor. Turgor loss may have been adaptive in minimizing shoot growth and stomatal conductance under hydraulically limiting circumstances.

**Key words:** *Artemisia tridentata*; cavitation; drought adaptation, *Artemisia tridentata*; hydraulic limitations; sagebrush; water relations.

### INTRODUCTION

Sagebrush (*Artemisia tridentata*) is emblematic of the arid Great Basin region of the United States. The shrub dominates over 150 000 km<sup>2</sup> of the landscape (McArthur and Ott 1996). Within its wide geographic range, sagebrush also has a broad ecological distribution from dry valley floors, where annual precipitation can be less than 160 mm per year, to mesic mountain tops with double or triple the valley precipitation (West 1983). Along this gradient are found three major subspecies (Cronquist 1994), ssp. *wyomingensis* at the low and dry end of the spectrum, ssp. *vaseyana* at the high and wet end, and ssp. *tridentata* intermediate (Fig. 1). Presumably, the morphological differences defining these taxa are associated with adaptive physiological differences. This paper examines physiological differences with respect to drought adaptation in *A. tridentata* subspecies.

Morphologically, the subspecies differ in stature, inflorescence structure, and ploidy levels. Subspecies

*wyomingensis* is short (<0.5 m) with floral stalks that arise throughout the crown, and is consistently tetraploid (McArthur et al. 1981). Subspecies *tridentata* is tall (generally >1.5 m in height) with floral stalks resembling those of ssp. *wyomingensis*. Plants of ssp. *tridentata* can be either diploid or tetraploid with no known morphological or ecological features distinguishing plants with different ploidy levels (McArthur et al. 1981). Subspecies *vaseyana* is intermediate in height, usually diploid, and is distinguished from the other subspecies by reproductive shoots that arise from the upper crown and extend above the vegetative structures, giving the plants a flat-topped appearance (McArthur et al. 1981). The differences in morphology between the subspecies are maintained in common garden, suggesting that they have a genetic basis (McArthur and Welch 1982, Barker and McKell 1986, Booth et al. 1990).

Few studies have evaluated physiological differences between the subspecies. Since the differences in habitat include major differences in soil water availability (Sturges 1979, Barker and McKell 1986) one would predict differences in drought adaptation between subspecies, with ssp. *wyomingensis* being the most drought-adapted and ssp. *vaseyana* being the least (Fig. 1). Comparative water relations of ssp. *wyomingensis*

Manuscript received 5 December 1997; revised 11 September 1998; accepted 28 September 1998; final version received 21 October 1998.

<sup>1</sup> Present address: Department of Biological Sciences, University of Arkansas, Fayetteville, Arkansas 72701 USA. E-mail: kkolb@comp.uark.edu

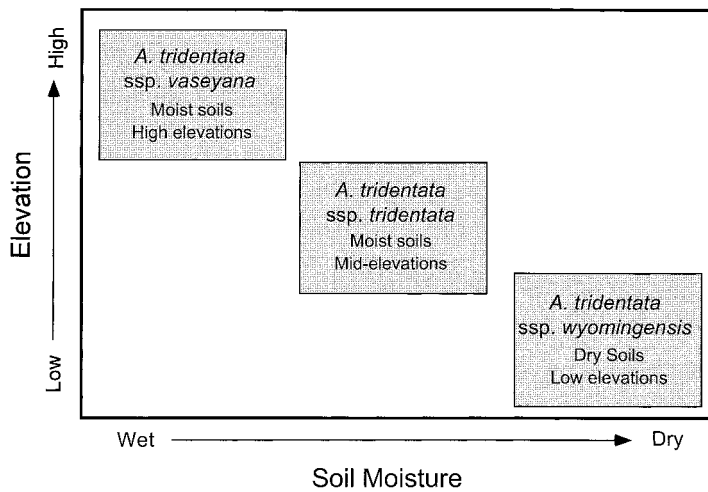


FIG. 1. Segregation of *Artemisia tridentata* subspecies along elevational and soil moisture gradients. Adapted from Hironaka (1978) and West (1983).

and *tridentata* growing contiguously in nature suggested little difference in functional rooting depth (Shumar and Anderson 1986). A common garden study found that ssp. *tridentata* had the highest rates of photosynthesis and highest  $\delta^{13}\text{C}$ , followed by ssp. *wyomingensis*, and that *vaseyana* had the lowest average values (Frank et al. 1984). Since  $\delta^{13}\text{C}$  values can be used as a proxy for water use efficiency, this suggests that the two low-elevation subspecies (ssp. *wyomingensis* and *tridentata*) were the most water use efficient, consistent with them occupying areas that are drier than ssp. *vaseyana*. However, patterns in  $\delta^{13}\text{C}$  differed between the 2 yr studied, and physiological distinctions between the subspecies remain ambiguous.

The present study evaluated the differences in drought experience and drought tolerance between the subspecies. Drought experience was quantified in terms of seasonal patterns of xylem pressure and transpiration rates in natural populations. Drought tolerance is a result of many traits, of which we focused on one, vulnerability to xylem cavitation. Xylem cavitation is the rupture of the water column held under negative pressure in the xylem. We emphasized cavitation because of its explicit link to the plant's potential for gas exchange; plants cannot conduct water if their xylem conduits are cavitated. As a secondary drought tolerance parameter, we quantified the turgor loss point. The turgor loss point is the water potential at which protoplasmic pressure reaches atmospheric. Its physiological significance is more ambiguous than cavitation resistance, with potential consequences including the inhibition of cell growth, disruption of tissue structure, and induction of stomatal closure (Kramer 1988, Schulze et al. 1988).

Our hypothesis was that the subspecies' vulnerability to cavitation and turgor loss points would differ according to the degree of drought they experienced, and that this would parallel the qualitative ranking shown in Fig. 1. Vulnerability to cavitation was measured in

both natural populations and a common garden population to evaluate genetic vs. environmental influence on the trait. In a theoretical discussion of the results, a model of the soil-plant continuum (Sperry et al. 1998; see Appendix) was used to determine the extent that differences in water use between subspecies could be linked to different hydraulic limitations imposed by cavitation.

## METHODS

### Study sites

Natural populations of *A. tridentata* were studied at three sites within 16 km of each other. These sites were in the vicinity of the East Tintic Mountains of central Utah. The ssp. *wyomingensis* site was at 1620 m (112°00' N, 39°57'30" W), the ssp. *tridentata* site was at 1780 m (112°10' N, 39°50' W), and the ssp. *vaseyana* site was at 2040 m (112°05' N, 39°57'30" W).

The common garden, containing all three subspecies, was located west of Nephi, Utah (111°47'30" N, 39°42'30" W) ~50 km from the natural populations at an elevation of 1562 m. The garden was established by the U.S. Forest Service Intermountain Research Station (Provo, Utah) in 1978. At the time of this study, all of the plants in the garden were adults that were originally established from seeds collected from their native populations, germinated in a greenhouse, and then transplanted into the garden. The accessions of ssp. *wyomingensis* were from a population in Millford, Utah. The ssp. *tridentata* plants were from Clear Creek and Dog Valley, Utah. The ssp. *vaseyana* material was from populations at Durkee Springs, Clear Creek, and Benmore, Utah. Vouchers of both native and common garden plants were filed in the Garret Herbarium of the University of Utah Museum of Natural History, Salt Lake City, Utah.

### Seasonal water relations

Seasonal trends in water relations were determined for ssp. *wyomingensis* and *vaseyana* in order to com-

TABLE 1. Abbreviations and definitions. Some additional symbols are confined to the Appendix and defined therein.

| Symbol        | Definition  | Units   |
|---------------|---|---|
| $A_x$         | functional xylem area                                 | $m^2$   |
| $A_l$         | one-sided leaf area                                   | $m^2$   |
| $A_r$         | absorbing root area                                   | $m^2$   |
| $E$           | transpiration rate                                    | $mmol \cdot s^{-1} \cdot m^{-2}$                |
| $E_{crit}$    | theoretical maximum $E$                               | $mmol \cdot s^{-1} \cdot m^{-2}$                |
| $k$           | hydraulic conductance = flow rate/pressure difference | $mmol \cdot s^{-1} \cdot MPa^{-1}$              |
| $k_h$         | hydraulic conductivity = flow rate/pressure gradient  | $mmol \cdot m^{-1} \cdot s^{-1} \cdot MPa^{-1}$ |
| branch $k_x$  | branch-specific conductivity = $k/A_x$                | $mol \cdot s^{-1} \cdot MPa^{-1} \cdot m^{-2}$  |
| segment $k_x$ | segment-specific conductivity = $k_h/A_x$             | $mol \cdot s^{-1} \cdot MPa^{-1} \cdot m^{-1}$  |
| $k_l$         | leaf-specific conductivity = $k/A_l$                  | $mmol \cdot s^{-1} \cdot MPa^{-1} \cdot m^{-2}$ |
| $\Psi_x$      | xylem pressure  | MPa   |
| $\Psi_{crit}$ | theoretical minimum leaf $\Psi_x$                     | MPa   |
| $\Psi_p$      | predawn leaf xylem pressure                           | MPa   |
| $\Psi_m$      | midday leaf xylem pressure                            | MPa   |
| $\Psi_{50}$   | xylem pressure at 50% cavitation                      | MPa   |
| $\Psi_{tip}$  | xylem pressure at turgor loss                         | MPa   |
| $\Psi_{sat}$  | osmotic potential at saturation                       | MPa   |
| $\Psi_s$      | soil water potential                                  | MPa   |

pare the drought experienced by the subspecies at elevational extremes (Fig. 1). The parameters measured were shoot xylem pressure ( $\Psi_x$ ) and shoot transpiration rate ( $E$ , see Table 1 for list of abbreviations). All parameters were measured at each site on two consecutive days in June, August, and November of 1996. These sampling dates were chosen because the majority of the precipitation within the Great Basin is received during the winter, resulting in a predictable summer drought. Therefore, a comparison of plant performance in June vs. August allowed us to determine the effect of the summer drought period. We sampled again in November following an unusually wet period (~60% above normal) between September and October in order to quantify whether or not there was any recovery from the drought.

Measurements of  $\Psi_x$  and  $E$  were conducted on five plants, with three replicates per plant for each measurement date. A pressure chamber (P.M.S. Instruments, Corvallis, Oregon, USA) was used to measure  $\Psi_x$  on small (<80 mm long) leafy shoot tips. Predawn xylem pressure ( $\Psi_p$ ) was measured between 0500 and 0630 and midday pressure ( $\Psi_m$ ) was taken between 1300 and 1400.

Transpiration rates were measured between 1100 and 1300 using a null balance porometer equipped with a cylindrical chamber to accommodate the leafy shoots of sagebrush (LI-1600m, LICOR Inc., Lincoln, Nebraska, USA). Transpiration was expressed per one-sided leaf area. Leaf areas were measured with a leaf area meter (LI-3100, LICOR Inc., Lincoln, Nebraska, USA). Porometer estimates of in situ  $E$  are subject to error because the cuvette environment may alter boundary layer conductance and leaf temperature (McDermitt 1990). However, these errors were relatively minor in our context because (1) leaves of sagebrush are small (0.26–1.23  $cm^2$ , Shultz 1986) resulting in a large boundary layer conductance relative to stomatal con-

ductance, and (2) ambient relative humidity was low (<25%) making it the dominant factor determining the evaporative gradient from leaf to air.

#### Hydraulic conductance expressions

The many expressions of hydraulic conductance used in this paper are summarized in Table 1. Hydraulic conductance ( $k$ ) was defined as the slope of the relationship between flow rate and the driving force. The driving force was either a difference in  $\Psi_x$ , or a difference between soil water potential ( $\Psi_s$ ) and  $\Psi_x$ . In most cases  $k$  was estimated from flow rate measured at a single  $\Psi$ , which assumed the flow rate vs.  $\Psi$  relationship under measurement conditions was linear and passed through the origin. Nonzero flow intercepts were encountered in some measurements and were taken into account. The  $k$  was measured or estimated over all or part of the soil–plant continuum, and as noted in Table 1, it was expressed in terms of leaf area (“leaf-specific conductivity,”  $k_l$ ), functional xylem area (“specific conductivity,”  $k_x$ ), and pressure gradient (“conductivity,”  $k_h$ ).

#### Seasonal measurements of hydraulic conductance and leaf area

Three measures of hydraulic conductance were used to characterize changes associated with the summer drought:  $k$ ,  $k_l$ , and  $k_x$  (Table 1). The leaf-specific hydraulic conductivity ( $k_l$ ) was calculated from  $E$  and  $\Psi_x$  measurements:

$$k_l = E/(\Psi_p - \Psi_m) \quad (1)$$

where  $\Psi_p$  was used as a proxy for  $\Psi_s$ , and  $E$  is measured under steady-state conditions. The  $k_l$  represented the hydraulic pathway from bulk soil to leaf. From the changes in leaf area during the drought, we also converted relative changes in  $k_l$  during the season to rel-

ative changes in hydraulic conductance ( $k$ ) over the same soil-to-leaf pathway.

Within the shoot system we measured the specific conductivity ( $k_x$ ) of excised branches. The "branch  $k_x$ " was defined as the hydraulic conductance of the branch divided by the basal area of the current year's xylem ( $A_x$ , Table 1). The xylem of sagebrush shoots is functional for only 1 yr, after which it becomes sealed off by an interxylary cork layer and becomes discolored (Diettert 1938; K. J. Kolb, *personal observation*). The area of the current year's xylem was measured using a microscope equipped with a drawing tube that allowed the tracing of xylem area on a digitizing tablet (Microplan II, DonSanto Corporation, Natick, Massachusetts, USA).

At each date, 15 branches ~6–8 mm in basal diameter were collected from each population and brought to the laboratory. Branches were ~0.3–0.5 m in length and represented ~20–80% of the distance traveled by water in the shoots of these small shrubs. The branch  $k$  was measured using the method of Kolb et al. (1996). In the laboratory, the branches were recut under water to remove any emboli induced by harvesting and then defoliated. The branch base was attached to a supply of filtered (0.2  $\mu\text{m}$ ) HCl solution (pH = 2) located on a balance. The branch, excepting the basal end, was sealed in a vacuum canister. The uptake rate of solution from the balance was measured at five or more partial vacuum pressures. The  $k$  was calculated as the slope of the flow rate vs. pressure relationship to account for nonzero flow intercepts (Kolb et al. 1996).

In addition to the measurement of branch  $k$ , the ratio of leaf area to functional xylem area was quantified for each branch. Leaf area was estimated by collecting all leaves from the excised branch and oven-drying them for a minimum of 24 h. The dry mass was determined and used to calculate leaf area using linear regressions that were previously determined for each subspecies. The functional xylem area was measured in the same manner as described for  $k_x$  determination. Changes in the leaf area to functional xylem area ratio during the study period primarily reflect changes in leaf area, since xylem production in *A. tridentata* in central Utah is generally completed by June.

#### *Vulnerability to cavitation*

We quantified the vulnerability to cavitation by measuring "vulnerability curves" (Tyree and Sperry 1988) of stem xylem. Vulnerability curves express cavitation in terms of a loss in hydraulic conductivity of xylem, as  $\Psi_x$  becomes progressively more negative. We used the centrifugal force method (Pockman et al. 1995, Alder et al. 1997) to generate negative  $\Psi_x$  in excised stem segments. Hydraulic conductivity was measured using a modification of the method of Sperry et al. (1988).

Branches were collected, wrapped in plastic to minimize desiccation, and brought to the laboratory. The

branches were recut under water to a length of either 257 mm or 146 mm (without major side branches) to fit two sizes of centrifuge rotors. The segments were inserted into a tubing manifold supplied with either filtered (0.2  $\mu\text{m}$ ) HCl solution (pH = 2), or deionized and filtered (0.2  $\mu\text{m}$ ) water. Previous work has shown no difference in cavitation or hydraulic conductance, whether water or HCl solution was used (Alder et al. 1997). Use of water required weekly sterilizing of tubing to avoid microbial growth that would otherwise clog xylem. Stem segments were flushed for 20 min with solution at high pressure (100 kPa) to remove any air emboli caused naturally or as a result of harvesting.

Hydraulic conductivity of a stem segment ( $k_h$ ) was defined as the flow rate through the stem divided by the pressure gradient (pressure drop per stem length [ $\Delta\Psi_x/\text{length}$ ], Table 1). We controlled the pressure gradient using a hydraulic head of ~7 kPa, and flow rate was measured by routing the stem effluent to a reservoir on an electronic balance (Sperry et al. 1988). To increase the accuracy of measurement we measured the flow rate intercept (at zero applied pressure) before and after measuring the pressure-induced flow. The flow rate intercept was averaged and subtracted from the pressurized flow rate to obtain an estimate of the net flow caused by applied pressure. The flow rate intercept was small (<0.05 mg/s) and usually negative, meaning water was leaving the balance reservoir and entering the stem. There are a number of potential causes for a negative intercept, including evaporation from the stem surface, osmotic or capillary water uptake by the tissue, and leaks from small side branches or leaf bases (if stems are below the balance reservoir level). In addition to correcting for the background flow, we minimized it by submerging stems in water during measurement, and adjusting the height of the water to near that of the balance reservoir.

Once its  $k_h$  had been measured, the segment was mounted in one of two custom-built centrifuge rotors (modified from Alder et al. 1997) for a Sorvall RC-5C centrifuge (Kendro Laboratory Products, Newton, Connecticut, USA). Information on the design and construction of these rotors is available from the second author on request. Segments were placed with their long axes centered on the rotor's center of rotation. The ends of the stem segments were immersed in water to prevent loss of water from the ends during spinning. Rotors held three segments at a time. Segments were spun for 3 min at speed, exposing the xylem water to negative pressure. The minimum  $\Psi_x$  was at the center of rotation, and was a function of the angular velocity and the distance from the center of rotation to the free surface of the water submerging the stem ends (see Alder et al. 1997).

After spinning, segments were mounted in the tubing manifold, and  $k_h$  was remeasured. The  $k_h$  values were stable, showing no tendency to increase as they would if the cavitating vessels were being refilled during mea-

surement (Alder et al. 1997). The process was continued, spinning to progressively more negative  $\Psi_x$ , until  $k_h$  approached zero. Vulnerability curves were plotted as the percentage loss in  $k_h$  vs.  $\Psi_x$ .

Vulnerability curves for native populations were measured for 8–12 plants of each subspecies in late June of 1996, after all the year's xylem had been produced. Native populations were checked again in July of 1997 to assess year-to-year variation in cavitation resistance. The vulnerability curves for the subspecies growing in the common garden were determined for six plants of each subspecies in mid-July of 1997.

#### *Xylem conduit anatomy*

To examine the relationship between cavitation resistance and conducting efficiency, we measured xylem conduit diameters in stem xylem of the subspecies. Diameters were measured in the current year's xylem of the segments from the vulnerability curve experiments. Transverse sections were made from each segment, and vessel lumen diameters measured with the microscope-digitizing tablet arrangement used in xylem area measurements. Vessel diameters were calculated as the diameter of a circle with an area equivalent to the vessel lumen cross section. Every vessel in a radial sector defined by rays was measured. For each stem, the mean diameter was determined based on at least 200 vessels.

We calculated a hydraulically weighted mean diameter based on the vessels' contribution to hydraulic conductance. To calculate the hydraulic mean, the total number of vessels ( $n$ ) is adjusted to reflect each vessel's contribution to total hydraulic conductance. A vessel's hydraulic contribution is proportional to its diameter ( $d$ ) raised to the fourth power according to the Hagen-Poiseuille law (Zimmermann 1983). Each vessel is therefore represented in the new distribution  $d^4$  times, and the adjusted total number of vessels is  $n = \Sigma d^4$ . The contribution of each vessel to the total sum of diameters is  $d^4 \times d$ , and the adjusted sum of all diameters is  $\Sigma d^5$ . The hydraulic mean diameter is  $\Sigma d^5 / \Sigma d^4$ . The hydraulic mean is preferable over other artificial methods of hydraulically weighting diameter distributions (e.g., Tyree et al. 1994).

The specific conductivity of the stem segments ("segment  $k_x$ ") was also measured. Segment  $k_x$  was calculated as the maximum (noncavitated) hydraulic conductivity ( $k_h$ ) divided by the area of functional xylem ( $A_x$ ).

#### *Turgor loss point*

The xylem pressure at turgor loss ( $\Psi_{tp}$ ) and osmotic potential at saturation ( $\Psi_{sat}$ ) were estimated for both ssp. *wyomingensis* and *vaseyana* using the pressure-volume technique (Tyree and Hammel 1972). Terminal shoots were collected concurrent with  $\Psi_p$  measurements at each of the sampling dates. We collected two shoots (0.10–0.15 m length) from each of seven dif-

ferent plants from both populations. To avoid oversampling of individual plants, the plants used for pressure-volume analyses were different from those used for  $\Psi_x$  and  $E$  measurements. Since it has been shown that rehydrating sagebrush changes the pressure-volume relationship (Evans et al. 1990), the shoots used for rehydration were different from those used for pressure-volume analysis. The cut ends of the rehydrated samples were supplied with distilled water for 4 h and covered with a plastic bag, and the saturated masses determined. The shoots were oven-dried at 70°C for over 24 h and the dry mass was measured. Mean fresh mass to dry mass ratios of the rehydrated samples were calculated and used to calculate the saturated mass of the samples used in the pressure-volume analysis, as described by Evans et al. (1990). The shoots used for pressure-volume analysis were supplied with distilled water for less than 15 min, its water potential determined, and the shoot weighed. Between measurements the shoots were allowed to dehydrate by transpiration on the bench top (Hinckley et al. 1980). Bulk tissue estimates of turgor loss point and osmotic potential at saturation were made using a computer program provided by P. J. Schulte (Schulte and Hinckley 1985).

#### *Statistical analysis*

Statistical analysis was made using JMP software (Version 3.1, SAS Institute Incorporated, Cary, North Carolina, USA) and SAS (version 6.12, SAS Institute Incorporated, Cary, North Carolina, USA). The comparisons of field parameters for ssp. *wyomingensis* and *vaseyana* were made using a two-way analysis of variance and a Fisher's least squared difference test. This combination was used for analyzing xylem pressures, leaf transpiration rates, branch-specific conductivity, leaf area/xylem area ratios, and tissue water relations parameters. For each stem used to construct the vulnerability curves, we fit the data with a Weibull curve (Rawlings and Cure 1985), and then calculated the xylem pressure resulting in 50% loss in hydraulic conductivity ( $\Psi_{50}$ ). The  $\Psi_{50}$  estimates were then compared between subspecies for the native populations and the common garden plants using a two-way analysis of variance and a Fisher's least squared means test. Additionally, the percent loss in hydraulic conductivity (% loss in  $k_h$ ) for the native populations were compared using a one-way analysis of variance for each pressure. Prior to the statistical analysis, % loss in  $k_h$  was arcsine transformed. Correlations between xylem anatomy parameters were statistically analyzed using Pearson correlation tests.

## RESULTS

### *Seasonal patterns in water relations and hydraulic conductance*

The  $\Psi_x$  data (Fig. 2A) for ssp. *wyomingensis* and *vaseyana* exhibited the expected seasonal trend, de-

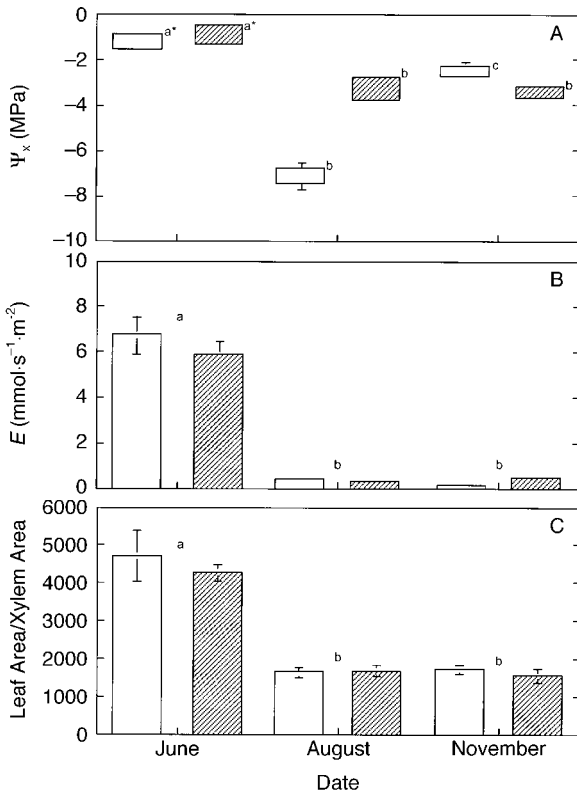


FIG. 2. Seasonal patterns of water relations and leaf area for *A. tridentata* ssp. *wyomingensis* (open bars) and ssp. *vaseyana* (hatched bars). (A) The range of leaf xylem pressure (upper end of bar is mean  $\Psi_p$ , and the lower end is mean  $\Psi_m$  [ $\pm 1$  SE]). (B) Transpiration rates,  $E$ . (C) Ratio of leaf area to xylem functional area,  $A_1/A_x$ . Error bars are  $\pm 1$  SE ( $n = 5$ ). An asterisk indicates a nonsignificant difference between subspecies for a given sampling date, and shared lowercase letters denote nonsignificant differences between dates. The different notation for panel A reflects the fact that the subspecies $\times$ date interaction was significant for  $\Psi_p$  ( $F = 116.49$ ,  $df = 2, 24$ ,  $P < 0.05$ ) and  $\Psi_m$  ( $F = 109.68$ ,  $df = 2, 24$ ,  $P < 0.05$ ). In the case of panel A, nonsignificant differences are indicated within a subspecies between sampling dates by use of the same letter.

creasing from high values in June to low values in August in response to the summer drought. The summer drought in 1996 was more extreme than usual, with precipitation for the months of July and August only 52% of normal in central Utah. As expected from its low elevation habitat (Fig. 1), *ssp. wyomingensis* developed much lower  $\Psi_x$  in August ( $\Psi_p = -6.8$  MPa,  $\Psi_m = -7.5$  MPa) than the high elevation *ssp. vaseyana* ( $\Psi_p = -2.7$  MPa,  $\Psi_m = -3.8$  MPa).

Both subspecies reduced  $E$  to similar minimal values in August ( $P = 0.437$ ) in response to the drought (Fig. 2B). In addition to closing stomata, both taxa shed between 60 and 65% of their leaf area between June and August based on their changes in leaf area per xylem area (Fig. 2C), assuming negligible xylem production in the interim.

The drought was also associated with a large de-

crease in hydraulic conductance. The  $k_l$  of the soil-to-leaf pathway (Fig. 3A) decreased by 92% in *ssp. wyomingensis* and 94% in *ssp. vaseyana* between June and August. The branch  $k_x$  (Fig. 3B) also showed a pronounced decline of  $\sim 65\%$  in the two subspecies. The smaller decline in branch  $k_x$  vs. soil-to-leaf conductance indicated a substantial loss of conductance in the belowground component of the continuum.

In November, the  $\Psi_x$  of *ssp. wyomingensis* rose from August values, presumably in response to the fall rains (Fig. 2A). At the same time, however, no recovery was evident for  $\Psi_x$  in *ssp. vaseyana*. In neither taxon did  $\Psi_x$  reach the predrought values of June, despite obviously wet surface soils. Either the rainwater did not fully penetrate the active rooting zone, or there was a major disequilibrium between  $\Psi_p$  and  $\Psi_s$  at this time. November  $E$  did not increase in either subspecies relative to August values (Fig. 2). This was partially the result of a lower evaporative gradient in November vs. August, but also because leaf conductance remained at (*ssp. wyomingensis*) or slightly above (*ssp. vaseyana*) August values (data not shown). The two measures of

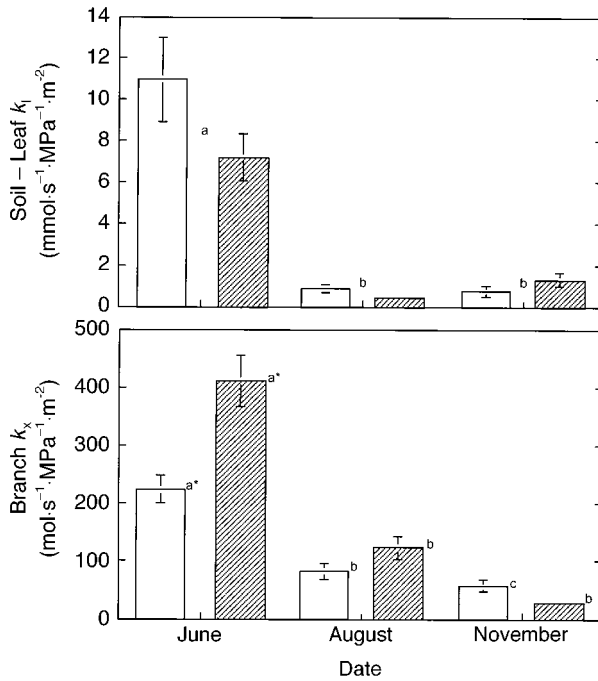


FIG. 3. Seasonal patterns of hydraulic conductance for *A. tridentata* ssp. *wyomingensis* (open bars) and ssp. *vaseyana* (hatched bars). (A) Leaf-specific hydraulic conductivity,  $k_l$ , from soil to leaf. (B) Specific conductivity of branch systems,  $k_x$ . Error bars are  $\pm 1$  SE ( $n = 5$  for  $k_l$ ,  $n = 15$  for  $k_x$ ). An asterisk indicates a significant difference between subspecies for a given sampling date, and shared lowercase letters denote nonsignificant differences between dates. The different notation for panel B reflects the fact that the subspecies $\times$ date interaction was significant for branch  $k_x$  ( $F = 11.14$ ,  $df = 2, 75$ ,  $P < 0.05$ ). In the case of panel B, nonsignificant differences are indicated within a subspecies between sampling dates by use of the same letter.

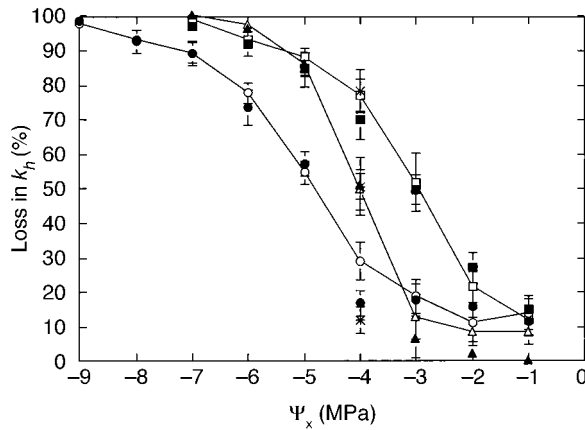


FIG. 4. Percentage loss in stem  $k_h$  vs.  $\Psi_x$  for the subspecies grown in native populations in 1996 (ssp. *wyomingensis*, open circles; ssp. *tridentata*, open triangles; ssp. *vaseyana*, open squares) and a common garden in 1997 (closed symbols). The percentage loss in  $k_h$  at  $\Psi = -4.0$  MPa measured in 1997 for each subspecies grown in native populations is also shown (\*). Error bars are  $\pm 1$  SE ( $n = 12$  for native populations of ssp. *wyomingensis* and *vaseyana*,  $n = 8$  for ssp. *tridentata*, and  $n = 6$  for common garden). The percentage loss in  $k_h$  was different between subspecies for all pressures below  $-3$  MPa ( $P < 0.05$ ). For each subspecies from native populations, there was no significant difference between the percentage loss in  $k_h$  at  $\Psi = -4.0$  MPa measured in 1996 and that measured in 1997 ( $P > 0.05$ ).

in situ hydraulic conductance ( $k_l$  and branch  $k_x$ ) also showed no recovery, but remained depressed below August values (Fig. 3). The decrease in branch  $k_x$  for both subspecies between August and November ( $P < 0.01$ ) may have been caused by freezing-induced cavitation because there were multiple freeze-thaw events in September at the ssp. *vaseyana* site (K. J. Kolb, unpublished data), and possibly also at the ssp. *wyomingensis* site.

*Vulnerability to cavitation*

The three subspecies differed substantially in their vulnerability to cavitation (Fig. 4), in agreement with their reputed drought tolerance ranking summarized in Fig. 1. Subspecies *wyomingensis* was the most resistant

to cavitation, having lost 50% of its conducting capacity at  $\Psi_{50} = -4.9$  MPa (Table 2), and maintaining hydraulic transport to below  $-9$  MPa (Fig. 4). In contrast, subspecies *vaseyana* was the most vulnerable to cavitation with a  $\Psi_{50}$  of  $-3.0$  MPa (Table 2), and the stems becoming completely cavitated by approximately  $-7$  MPa (Fig. 4). The cavitation response for ssp. *tridentata* was intermediate, with a  $\Psi_{50}$  of  $-3.9$  MPa (Table 2). The  $\Psi_{50}$  estimates for the three subspecies were significantly different ( $F = 25.67$ ,  $df = 2, 43$ ,  $P < 0.05$ ; Table 2). There was no significant effect of the interaction between subspecies and sampling date ( $F = 0.10$ ,  $df = 2, 43$ ,  $P = 0.9029$ ), nor were there any significant differences between  $\Psi_{50}$  estimated for the native vs. common garden plants ( $F = 0.67$ ,  $df = 1, 43$ ,  $P = 0.4178$ ). Furthermore, there was no evidence for year-to-year variation in cavitation resistance, as the % loss in  $k_h$  of stems spun at  $-4$  MPa measured in July of 1997 was not significantly different from that measured in July of 1996 (Fig. 4, open squares).

Based on the decrease in  $\Psi_m$  between June and August (Fig. 2A), a loss in stem conductivity of 88 and 63% was predicted, based on the vulnerability curves for ssp. *wyomingensis* and *vaseyana*, respectively (Fig. 4). For comparison, the in situ loss in branch  $k_x$  was 65 and 70%, respectively (Fig. 3B). The comparison is approximate because branch  $k_x$  measurement included the entire branch system while the vulnerability curve only represented stem segments.

The vulnerability curves of the common garden plants were not different from those collected from native populations (Fig. 4, compare open vs. solid symbols), suggesting that the intraspecific variation in cavitation resistance was a result of genetic differentiation rather than phenotypic plasticity.

*Mean vessel diameters*

Vessel diameter, hydraulically weighted diameter, and stem segment  $k_x$  were not significantly different between common garden vs. native populations, with the single exception of hydraulic mean diameter for ssp. *vaseyana* ( $P = 0.0006$  for ssp. *vaseyana* hydraulic diameters). Using the pooled data (Table 2), hydraulic

TABLE 2. Functional xylem parameters for the three subspecies of *A. tridentata*.

| Subspecies          | Hydraulic diameter ( $\mu\text{m}$ ) | Diameter ( $\mu\text{m}$ )   | Segment $k_x$ ( $\text{mol}\cdot\text{s}^{-1}\cdot\text{MPa}^{-1}\cdot\text{m}^{-1}$ ) | $\Psi_{50}$ (MPa)           |
|---------------------|--------------------------------------|------------------------------|--|-----------------------------|
| <i>wyomingensis</i> | 26.5 <sup>a</sup> $\pm$ 0.1          | 21.4 <sup>a</sup> $\pm$ 0.9  | 27.7 <sup>a</sup> $\pm$ 4.3  | -4.9 $\pm$ 0.1 <sup>a</sup> |
| <i>tridentata</i>   | 25.2 <sup>a</sup> $\pm$ 0.6          | 19.6 <sup>ab</sup> $\pm$ 0.4 | 50.9 <sup>b</sup> $\pm$ 7.7  | -3.9 $\pm$ 0.1 <sup>b</sup> |
| <i>vaseyana</i>     | 33.0 <sup>b</sup> $\pm$ 1.3          | 22.8 <sup>ac</sup> $\pm$ 2.8 | 40.3 <sup>ab</sup> $\pm$ 6.6   | -3.0 $\pm$ 0.1 <sup>c</sup> |

Notes: Means of the pooled native and common garden data for hydraulically weighted diameters (hydraulic diameter), nonweighted diameters (diameter), and the specific conductivity of stem segments (segment  $k_x$ )  $\pm 1$  SE ( $n = 17$  for ssp. *wyomingensis*,  $n = 14$  for ssp. *tridentata*, and  $n = 18$  for ssp. *vaseyana*). The mean xylem pressure causing 50% loss ( $\Psi_{50}$ ) in hydraulic conductivity is also shown for the three subspecies ( $n = 11$  for ssp. *wyomingensis*,  $n = 12$  for ssp. *vaseyana*, and  $n = 8$  for ssp. *tridentata*). Means with the same letter within a column do not differ significantly ( $P > 0.05$ ).

TABLE 3. Mean xylem pressure at turgor loss ( $\Psi_{tp}$ ) and osmotic potential at saturation ( $\Psi_{sat}$ ) of *A. tridentata* ssp. *wyomingensis* and *vaseyana* for each of the sampling dates.

| Subspecies          | Sampling date | $\Psi_{tp}$ (MPa) | $\Psi_{sat}$ (MPa) |
|---------------------|---------------|-------------------|--------------------|
| <i>wyomingensis</i> | June          | $-2.4 \pm 0.1$    | $-1.2 \pm 0.1$     |
|                     | August        | $-4.6 \pm 0.6$    | $-3.7 \pm 0.4$     |
|                     | November      | $-2.6 \pm 0.2$    | $-2.0 \pm 0.2$     |
| <i>vaseyana</i>     | June          | $-1.7 \pm 0.1$    | $-1.4 \pm 0.1$     |
|                     | August        | $-3.4 \pm 0.3$    | $-2.4 \pm 0.2$     |
|                     | November      | $-2.7 \pm 0.1$    | $-2.3 \pm 0.1$     |

Notes: Values are means  $\pm$  1 SE ( $n = 6$ ). The  $\Psi_{tp}$  was different between subspecies and between all sampling dates (Fisher's least squared difference test,  $P < 0.05$ ) However,  $\Psi_{sat}$  was different only between sampling dates (Fisher's least squared difference test,  $P < 0.05$ ).

mean diameter was largest in ssp. *vaseyana* ( $P < 0.0001$ ) and segment  $k_x$  was lowest in ssp. *wyomingensis* ( $P = 0.0078$ ).

Based on individual stem segments (not pooled by subspecies), hydraulic mean diameter was positively correlated with  $\Psi_{50}$  ( $r = 0.53$ ,  $P < 0.01$ ), suggesting that larger vessels were associated with less negative cavitation pressures across all subspecies and sites. The correlation was strongest within common garden data ( $r = 0.69$ ,  $P < 0.01$ ). There were no correlations between segment  $k_x$  and  $\Psi_{50}$ , or  $k_x$  and hydraulic mean diameter, except for rather weak relationships within the common garden data ( $r = 0.54$ ,  $P < 0.05$ ;  $r = 0.51$ ,  $P < 0.05$ , respectively).

Turgor loss points

Subspecies *wyomingensis* had a lower turgor loss point than ssp. *vaseyana* for all sampling periods (Table 3). Both subspecies exhibited lower turgor loss points and saturated osmotic potentials in response to the summer drought. In August,  $\Psi_p$  and  $\Psi_m$  were below the turgor loss point, indicating that seasonal osmotic adjustment was not sufficient to maintain turgor during the summer drought period. In November, both  $\Psi_p$  and  $\Psi_m$  recovered to near the predrought values and were accompanied by an increase in the  $\Psi_{tp}$  to near the June values, implying that leaves had regained positive turgor potentials.

DISCUSSION

Analysis of hydraulic limits

Both ssp. *wyomingensis* and *vaseyana* showed similar reduction in water use based on their equivalent reductions in leaf area and  $E$  (Fig. 2B,C), despite the fact that ssp. *wyomingensis* fell to much lower  $\Psi_x$  than ssp. *vaseyana* during drought (Fig. 2A). One adaptive explanation for the similar drought responses is that they were required to avoid hydraulic failure by cavitation. Based on the vulnerability curves, hydraulic failure should occur at a higher  $\Psi_x$  for ssp. *vaseyana* than ssp. *wyomingensis* (Fig. 4). We undertook a the-

oretical evaluation of this hypothesis by applying a model for hydraulic failure in the soil-plant continuum (Sperry et al. 1998) to the subspecies data (see Appendix).

Each curve in Fig. 5 is the relationship between  $E$  and leaf  $\Psi_x$  predicted by the model for a given bulk soil  $\Psi$  (the x axis intercept). The curves were fit to measurements of  $\Psi_p$  (proxy of bulk soil  $\Psi$ ),  $\Psi_m$ , and  $E$ , for June (solid circles) and August (open circles) data. As  $E$  is increased from zero in these curves, there is a disproportionate decrease in leaf  $\Psi_x$  because of the loss of hydraulic conductance in the continuum. Two sources of this loss in conductance loss were modeled, xylem cavitation, and soil drying in the rhizosphere (Newman 1969, Bristow et al. 1984; Appendix). The maximum permissible  $E$  ( $E_{crit}$ ) is associated with a minimum leaf  $\Psi_x$  ( $\Psi_{crit}$ ). If the plant increases  $E$  above  $E_{crit}$ , hydraulic failure occurs because the hydraulic conduc-

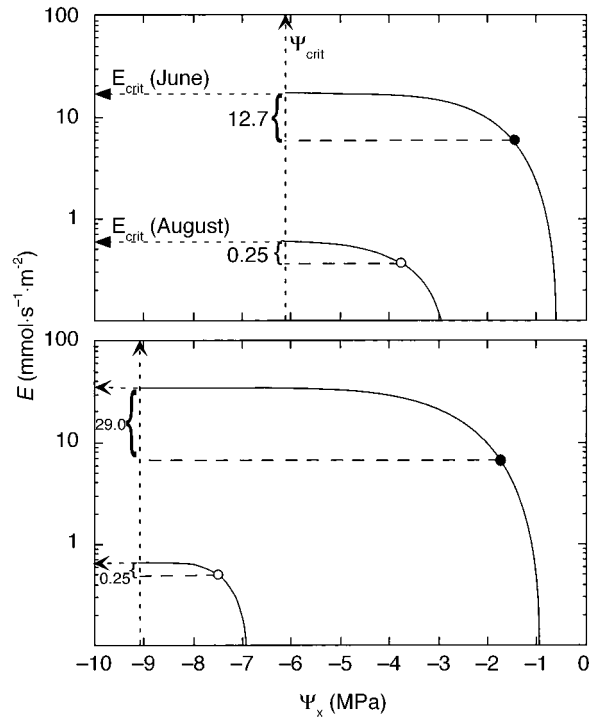


FIG. 5. Modeled transpiration rate ( $E$ ) vs. leaf  $\Psi_x$  for *A. tridentata* ssp. *wyomingensis* and ssp. *vaseyana* (panels A and B, respectively) for the June (solid curve with filled circle) vs. August (solid curve with open circle) sampling dates. Within each panel, the  $\Psi$  intercept at  $E = 0$  represents  $\Psi_p$ , the circle is midday  $E$  at  $\Psi_m$ , and the values represent the safety margins from maximum transpiration ( $E_{crit} - E$ ) for June and August. The maximum transpiration rate ( $E_{crit}$ ) decreased with drought, but the associated minimum leaf  $\Psi_x$  ( $\Psi_{crit}$ ) was constant and approximated the 100% cavitation pressure (Fig. 4). The greater resistance of ssp. *wyomingensis* to cavitation was associated with a lower  $\Psi_{crit}$ . In both subspecies, the safety margin from  $E_{crit}$  decreased with drought to minimal values of a few tenths of a millimole per second per square meter. August  $\Psi_x$  for ssp. *wyomingensis* was below  $\Psi_{crit}$  for ssp. *vaseyana*.



TABLE 4. Selected parameters and outputs of the hydraulic failure analysis.

| Subspecies          | $A_r:A_l$ |        | Loss in $A_r$ ,<br>predicted (%) | Loss in $k$ (%) |          |
|---------------------|-----------|--------|----------------------------------|-----------------|----------|
|                     | June      | August |                                  | Predicted       | Measured |
| <i>wyomingensis</i> | 12        | 20     | 42                               | 96              | 97       |
| <i>vaseyana</i>     | 6         | 0.4    | 98                               | 69              | 98       |

Note:  $A_r:A_l$  is the root area to leaf area ratio required to fit the model to measured values of  $\Psi_p$ ,  $\Psi_m$ , and  $E$ . Predicted percentage loss of  $A_r$  is the loss of absorbing root area between June and August based on the change in  $A_r:A_l$  and the measured loss of  $A_l$  (Fig. 2C). The predicted percentage loss in  $k$  is calculated from the change in soil-leaf  $k$  between June and August from the model. The measured percentage loss in  $k$  is based on the change in  $k_l$  measured between June and August corrected for the loss of  $A_l$  (Fig. 2B, C).

tance of the continuum becomes zero either in xylem or rhizosphere (Sperry et al. 1998). The safety margin of the plant from failure can be predicted from the proximity of measured  $E$  and  $\Psi_x$  to  $E_{crit}$  and  $\Psi_{crit}$ .

The model predicted hydraulic failure to occur in the xylem rather than the rhizosphere, because  $\Psi_{crit}$  values (Fig. 5) approximated the xylem pressure required to cause 100% cavitation in the xylem (Fig. 4). If hydraulic failure had occurred in the rhizosphere,  $\Psi_{crit}$  would have been less negative (Sperry et al. 1998). Significantly, both the predawn and midday xylem pressures in ssp. *wyomingensis* in August were below  $\Psi_{crit}$  for ssp. *vaseyana*. As expected, when we tried to obtain a model fit to August data for ssp. *wyomingensis* while using the cavitation resistance of ssp. *vaseyana*, the model found no solution. This strengthens the conclusion that ssp. *vaseyana* could not obtain water under the drought conditions endured by ssp. *wyomingensis*, because its xylem would not be sufficiently resistant to cavitation.

Safety margins from  $E_{crit}$  in both subspecies showed a substantial decrease from relatively large values in June (13–29 mmol·s<sup>-1</sup>·m<sup>-2</sup>), to low values in August (0.25 mmol·s<sup>-1</sup>·m<sup>-2</sup>, Fig. 4). Although ssp. *vaseyana* was at a soil water potential 4 MPa higher than ssp. *wyomingensis* during the drought, its  $E$  was similarly constrained because of its greater vulnerability to cavitation. If  $E$  had not been reduced as soil drought progressed, it would have exceeded  $E_{crit}$ . The results provide theoretical support for the hypothesis that the decrease in  $E$  observed in both species was necessary to avoid hydraulic failure by cavitation.

The model can be evaluated by comparing predicted vs. measured loss of hydraulic conductance in the soil-leaf continuum from June to August (Table 4). Agreement was good in ssp. *wyomingensis* with 96 (predicted) vs. 97% (measured) loss of conductance. However, agreement was not as good for ssp. *vaseyana* with only 69% predicted loss of conductance vs. the measured 98%. Apparently, the model was missing a more hydraulically constraining component for ssp. *vaseyana*. We suspect the root xylem in ssp. *vaseyana* is significantly more vulnerable than the stem xylem, as was the case in another sagebrush population that is

intermediate between ssp. *wyomingensis* and *vaseyana* (K. J. Kolb and J. S. Sperry, unpublished data).

The model prediction of the ratio of absorbing root area to leaf area ( $A_r:A_l$ , Appendix) also provides insight into its validity. The predrought (June)  $A_r:A_l$  for both subspecies (Table 4) was six for ssp. *vaseyana* and 12 for ssp. *wyomingensis*. These are in the upper part of the published range (Rendig and Taylor 1989, Glinski and Lipiec 1990) as would be expected for a drought-adapted species. Also expected is the higher  $A_r:A_l$  in ssp. *wyomingensis* which is more drought tolerant. The  $A_r:A_l$  should increase during drought because of the loss of leaf area (Fig. 2C). This was predicted for ssp. *wyomingensis*, although the increase from 12 to 20 was not as much as expected based on leaf loss alone, hence a 42% decrease in absorbing root area was indicated (Table 4). In contrast, the model predicted a drastic reduction in  $A_r:A_l$  during drought in ssp. *vaseyana* despite its loss of leaf area, implying a large and generally unrealistic 98% loss in absorbing root area (Table 4). This inconsistency was symptomatic of the model's underestimate of the loss of conductance. Adding a more vulnerable xylem component to the model for ssp. *vaseyana* corrected the discrepancy (results not shown).

#### General discussion

Our results show differences in drought adaptation between the subspecies of *A. tridentata* that may contribute to their localization along a gradient in water availability. Subspecies *wyomingensis* experienced a leaf  $\Psi_x$  more than 3.5 MPa below ssp. *vaseyana* during the summer drought (Fig. 2A). The xylem of ssp. *wyomingensis* was also 1.9 MPa more resistant to cavitation than that of ssp. *vaseyana*, and 1 MPa more resistant than ssp. *tridentata* (Table 2).

These pronounced differences appeared to reflect genetic differentiation between the subspecies based on the common garden experiments, and the consistency in the percent loss measured at -4 MPa between different years (Fig. 4). Importantly, our results imply that neither ssp. *tridentata* nor *vaseyana* would be able to conduct water at the xylem pressures experienced by ssp. *wyomingensis* in August, because they would be

completely cavitated. Thus, the greater resistance to cavitation in ssp. *wyomingensis* appears to be a necessary adaptation for it to occupy the low-elevation, water-stressed habitat.

As suggested by the modeling exercise, vulnerability curves in these subspecies appear to be correlated to the range of soil water potentials experienced by the population, requiring comparable regulation of water use to remain with hydraulic limits. To achieve this by genetic differentiation would require strong stabilizing selection that makes the xylem sufficiently resistant to cavitation within a habitat on the one hand, while preventing it from becoming overly resistant on the other.

While it is easy to understand how the avoidance of hydraulic failure would be a powerful selective pressure against overly vulnerable xylem, it is more difficult to explain the selective disadvantage of overly resistant xylem. The leading hypothesis is that resistant xylem is also hydraulically inefficient xylem. This is supported by a weak correlation between increasingly negative  $\Psi_{50}$  and decreasing conduit diameter across a wide range of species (Tyree et al. 1994). Although we also saw this correlation across the subspecies, there was no relationship between cavitation resistance and segment  $k_x$ , which is an empirical measure of conducting efficiency. Although there is substantial evidence that cavitation is caused by the aspiration of air through interconduit pit membranes (Crombie et al. 1985, Tyree et al. 1994, Sperry et al. 1996), the link between cavitation resistance, conduit diameter, and conducting efficiency remains complex and requires more analysis.

The differences in turgor loss point (Table 3) between ssp. *wyomingensis* and *vaseyana* were also correlated with their drought exposure. While both taxa adjusted their turgor loss points during the drought (see also Evans et al. 1992), neither were able to maintain turgor. Unlike a complete loss of hydraulic conductance, the loss of turgor is apparently not maladaptive, because it probably occurs annually in the subspecies during the summer drought. Turgor loss may be part of the signaling pathway linking water stress to the shutdown of shoot growth and stomatal conductance. The link is complex, however, because both growth and stomatal conductance can bear an ambiguous relationship to bulk leaf turgor (Kramer 1988, Schulze et al. 1988). For example, in our study,  $E$  (a proxy for stomatal conductance) continued despite the apparent loss of turgor pressure in the bulk of the leaf tissue.

The discovery of substantial and apparently genetically based differences in cavitation resistance between closely related intraspecific taxa underscores the importance of this trait for adaptation to water availability. Strong selective pressures must be operating to generate and maintain these differences. Cavitation resistance may take on additional importance if rooting depths do not differ substantially between subspecies, as suggested by Shumar and Anderson (1986). Since

functionally related traits will likely evolve in concert, it is not surprising that the differences in cavitation resistance were associated with adjustments in turgor maintenance, leaf and plant size (McArthur and Welch 1982, Barker and McKell 1986), growth rate potential (Booth et al. 1990), and possibly water use efficiency (Frank et al. 1984). Sagebrush's domination of a broad elevational range in the Great Basin is associated with considerable adaptive variation in both physiological and morphological traits related to water use.

#### ACKNOWLEDGMENTS

This work was supported by the National Science Foundation grant IBN931980. We thank Durant McArthur of the USDA Intermountain Shrub Science Laboratory for his help in identifying the subspecies of sagebrush and graciously allowing us to use his common gardens, Nathan Alder for his assistance with data collection, the University of Utah Department of Biology for logistical support, and the Chief Consolidated Mining Company for allowing us to work on their property. Lynette Duncan of the University of Arkansas aided substantially in the statistical analyses. The authors also acknowledge the useful comments of the editor and two anonymous reviewers.

#### LITERATURE CITED

- Alder, N. N., W. T. Pockman, J. S. Sperry, and S. Nuismer. 1997. Use of centrifugal force in the study of xylem cavitation. *Journal of Experimental Botany* **48**:665–674.
- Barker, J. R., and C. M. McKell. 1986. Differences in big sagebrush (*Artemisia tridentata*) plant stature along soil-water gradients: genetic components. *Journal of Range Management* **39**:147–151.
- Booth, G. B., B. L. Welch, and T. L. C. Jacobson. 1990. Seedling growth rate of 3 subspecies of big sagebrush. *Journal of Range Management* **43**:432–436.
- Bristow, K. L., G. S. Campbell, and C. Calissendorff. 1984. The effects of texture on the resistance to water movement within the rhizosphere. *Soil Science Society of America Journal* **48**:266–270.
- Campbell, G. S. 1985. *Soil physics with basic; transport models for soil-plant systems*. Elsevier, Amsterdam, The Netherlands.
- Crombie, D. S., H. F. Hipkins, and J. A. Milburn. 1985. Gas penetration of pit membranes in the xylem of *Rhododendron* as the cause of acoustically detected sap cavitation. *Australian Journal of Plant Physiology* **12**:445–453.
- Cronquist, A. 1994. *Intermountain flora: vascular plants of the Intermountain West, USA*. Volume 5. New York Botanical Garden Press, Bronx, New York, USA.
- Diettert, R. A. 1938. The morphology of *Artemisia tridentata* Nutt. *Llyodia* **1**:3–74.
- Evans, R. D., R. A. Black, and S. O. Link. 1990. Rehydration-induced changes in pressure-volume relationships of *Artemisia tridentata* Nutt. ssp. *tridentata*. *Plant, Cell and Environment* **13**:455–461.
- Evans, R. D., R. A. Black, W. H. Loescher, and R. J. Fellows. 1992. Osmotic relations of the drought-tolerant shrub *Artemisia tridentata* in response to water stress. *Plant, Cell and Environment* **15**:49–59.
- Frank, C. T., B. N. Smith, and B. L. Welch. 1984. Photosynthesis, growth, transpiration, and  $\delta^{13}\text{C}$  relationships among three subspecies of big sagebrush (*Artemisia tridentata* Nutt.). Pages 332–335 in E. D. McArthur and B. L. Welch, editors. *Proceedings of the Symposium on the Biology of Artemisia and Chrysothamnus*. U.S. Forest Service Intermountain Research Station Technical Report **INT-GTR-200**.
- Glinski, J., and J. Lipiec. 1990. Soil physical conditions and

- plant roots. Chemical Rubber Company, Boca Raton, Florida, USA.
- Hinckley, T. M., F. Duhme, A. R. Hinckley, and H. Richter. 1980. Water relations of drought-hardy shrubs: osmotic potential and stomatal reactivity. *Plant, Cell and Environment* **3**:131–140.
- Hironaka, M. 1979. Basic synecological relationships of the Columbia River sagebrush type. Pages 27–32 in *The Sagebrush Ecosystem: a Symposium*. Logan, Utah, USA.
- Kolb, K. J., J. S. Sperry, and B. B. Lamont. 1996. A method for measuring xylem hydraulic conductance and embolism in entire root and shoot systems. *Journal of Experimental Botany* **47**:1805–1810.
- Kramer, P. J. 1988. Changing concepts regarding plant water relations. *Plant, Cell and Environment* **11**:565–568.
- McArthur, E. D., and J. E. Ott. 1996. Potential natural vegetation in the 17 conterminous Western United States. Pages 16–28 in J. R. Barrow, E. D. McArthur, R. E. Tausch, and J. Robin, editors. *Proceedings of the Symposium on Shrubland Ecosystem Dynamics in a Changing Environment*. U.S. Forest Service, Intermountain Research Station Technical Report **INT-GTR-338**.
- McArthur, E. D., C. L. Pope, and D. C. Freeman. 1981. Chromosomal studies of subgenus *Tridentatae* of *Artemisia*: evidence for autopolyploidy. *American Journal of Botany* **68**:589–605.
- McArthur, E. D., and B. L. Welch. 1982. Growth rate differences among big sagebrush (*Artemisia tridentata*) accessions and subspecies. *Journal of Range Management* **35**:396–401.
- McDermitt, D. K. 1990. Sources of error in the estimation of stomatal conductance and transpiration from porometer data. *HortScience* **25**:1538–1548.
- Newman, E. I. 1969. Resistance to water flow in soil and plant. I. Soil resistance in relation to amounts of root: theoretical estimates. *Journal of Applied Ecology* **6**:1–12.
- Passioura, J. B., and I. R. Cowan. 1968. On solving the non-linear diffusion equation for the radial flow of water to roots. *Agricultural Meteorology* **5**:129–134.
- Pockman, W. T., J. S. Sperry, and J. W. O'Leary. 1995. Sustained and significant negative pressure in xylem. *Nature* **378**:715–716.
- Rawlings, J. O., and W. W. Cure. 1985. The Weibull function as a dose-response model to describe ozone effects on crop yields. *Crop Science* **25**:807–814.
- Rendig, V. V., and H. M. Taylor. 1989. *Principles of soil-plant interrelationships*. McGraw Hill, New York, New York, USA.
- Schultze, E. D., E. Steudle, T. Gollan, and U. Schurr. 1988. Response to Dr. P. J. Kramer's article, "Changing concepts regarding plant water relations, Volume 11, Number 7, pp. 565–568." *Plant, Cell and Environment* **11**:573–576.
- Shultz, P. O., and T. M. Hinkley. 1985. A comparison of pressure-volume curve data analysis techniques. *Journal of Experimental Botany* **36**:1590–1602.
- Shultz, L. M. 1986. Comparative leaf anatomy of sagebrush: ecological considerations. Pages 253–264 in E. D. McArthur and B. Welch, editors. *Proceedings of the symposium on the biology of Artemisia and Chrysothamnus*. U.S. Forest Service, Intermountain Research Station Technical Report **INT-200**.
- Shumar, M. L., and J. E. Anderson. 1986. Water relations of two subspecies of big sagebrush on sand dunes in South-eastern Idaho. *Northwest Science* **60**:179–185.
- Sperry, J. S., F. R. Adler, G. S. Campbell, and J. C. Comstock. 1998. Hydraulic limitation of flux and pressure in the soil-plant continuum: results from a model. *Plant, Cell and Environment* **21**:347–359.
- Sperry, J. S., J. R. Donnelly, and M. T. Tyree. 1988. A method for measuring hydraulic conductivity and embolism in xylem. *Plant, Cell and Environment* **83**:414–417.
- Sperry, J. S., N. Z. Saliendra, W. T. Pockman, H. Cochard, P. Cruiziat, S. D. Davis, F. W. Ewers, and M. T. Tyree. 1996. New evidence for large negative pressures and their measurement by the pressure chamber method. *Plant, Cell and Environment* **19**:427–436.
- Sturges, D. L. 1979. Hydrologic relations of sagebrush lands. Pages 86–100 in *The Sagebrush Ecosystem: a symposium*. Logan, Utah, USA.
- Tyree, M. T., S. D. Davis, and H. Cochard. 1994. Biophysical perspectives of xylem evolution: is there a trade-off of hydraulic efficiency for vulnerability to dysfunction? *International Association of Wood Anatomists Bulletin* **15**:335–360.
- Tyree, M. T., and H. T. Hammel. 1972. The measurement of the turgor pressure and the water relations of plants by the pressure-bomb technique. *Journal of Experimental Botany* **23**:267–282.
- Tyree, M. T., and J. S. Sperry. 1988. Do woody plants operate near the point of catastrophic xylem dysfunction caused by dynamic water stress? *Plant Physiology* **88**:574–580.
- West, N. E. 1983. Great Basin-Colorado Plateau sagebrush semi-desert. Pages 331–349 in N. E. West, editor. *Ecosystems of the world: temperate deserts and semi-deserts Volume 5*. Elsevier, New York, New York, USA.
- Zimmermann, M. H. 1983. *Xylem structure and the ascent of sap*. Springer-Verlag, Berlin, Germany.

APPENDIX

MODELING HYDRAULIC LIMITATIONS

The model solved Eq. 1 for the relationship between  $E$  and leaf  $\Psi_x$  under steady-state conditions, with the assumption that  $\Psi_p$  = bulk soil matric potential (osmotic effects were ignored). The hydraulic conductance was a function of  $\Psi$  according to vulnerability curves for plant xylem and soil characteristics for the rhizosphere. To run the model,  $E$  was incremented from zero and Eq. 1 solved for steady-state  $\Psi$  and  $k$  at each increment until no solution existed because  $k = 0$  (Fig. 5). The  $E_{crit}$  was the maximum permissible  $E$  (Fig. 5), and was associated with a limiting leaf  $\Psi_x$  ( $\Psi_{crit}$ ).

To solve Eq. 1, the continuum was divided into a linear series of conducting elements. The model required only as many elements as there were  $k(\Psi)$  functions in the continuum (Sperry et al. 1998). The plant was characterized by one  $k(\Psi)$  function, the vulnerability curve of stem xylem. We used a Weibull function (Rawlings and Cure 1985) to fit a curve to vulnerability data (see Fig. 4), which gives the following  $k(\Psi)$  function:

$$k_p = k_p^* e^{-(\Psi/d)^c} \tag{A.1}$$

where  $k_p$  is the hydraulic conductance from root-to-leaf,  $k_p^*$  is the corresponding predrought (i.e., maximum) conductance, and  $d, c$  are curve-fitting parameters. Plant conductances were expressed per leaf area, and  $k_p^*$  was set to the mean  $k_l$  measured in June. When the model was run for August conditions, the maximum  $k_l$  value was adjusted upward in proportion to the amount of leaf area lost between June and August (Fig. 2C).

The rhizosphere component of the model required more elements because the assumed cylindrical geometry of water uptake into roots created a continuum of  $k(\Psi)$  functions. The rhizosphere width (bulk soil to root surface) was set to 5 mm, and divided into 11 elements using a log transformation (Pasioura and Cowan 1968) to set element lengths exponentially smaller near the root surface where  $\Psi_s$  gradients are largest. The  $k(\Psi)$  function for each element  $i$  was as given in the following equation (Eq. A.2) (Campbell 1985):

$$k_{si} = X_i K_s^* (\Psi_e/\Psi_1)^{(2+3/b)} \tag{A.2}$$

where  $k_{si}$  is the conductance of element  $i$ ,  $X_i$  is a conductance factor derived from the cylindrical geometry of uptake,  $K_s^*$  is the saturated soil conductivity ( $\text{mol}\cdot\text{s}^{-1}\cdot\text{MPa}^{-1}\cdot\text{m}^{-1}$ ),  $\Psi_e$  is the air entry potential for the soil, and  $b$  is a parameter derived from soil texture (Campbell 1985). Soil parameters are shown in Table A1 and were calculated according to Campbell (1985) from sand, silt, and clay fractions measured on three samples per site taken at  $\sim 30\text{-cm}$  depth (Table A1). Samples were analyzed with the hydrometer method by the Utah State University Soil Analytical Laboratory at Logan, Utah. The conductance factor  $X_i$  depended on the total root length ( $l$ ):

$$X_i = 2\pi l/\ln(r_i + 1/r_i) \tag{A.3}$$

where  $r_i$  is the radius of element  $i$  (Campbell 1985). Rhizosphere conductance was expressed on a root area basis by assuming a root radius of 0.1 mm for absorbing roots.

The model required an estimate of the ratio of absorbing root area to transpiring leaf area ( $A_r:A_l$ ) in order to couple the conductances in the rhizosphere (expressed per root area) with those in the plant (expressed per leaf area). The  $A_r:A_l$  was not measured, but iteratively adjusted to fit the model to the data as explained below. Leaf area in the model was arbitrarily set to 1 m<sup>2</sup> for June data, and was adjusted down according to the measured reduction in leaf area (Fig. 2C) for the August data. The actual values of leaf area did not matter because model results were expressed on a leaf area basis or as the percent change associated with drought.

To predict hydraulic safety margins, we ran the model for June and August measurements of  $\Psi_p$  and  $\Psi_m$ . The model predicted an  $E$  value from the  $\Psi_p$  and  $\Psi_m$  data, and iteratively adjusted  $A_r:A_l$  until the predicted  $E$  matched the measured  $E$ . The associated  $E_{crit}$  and  $\Psi_{crit}$  were used to determine proximity of the plant to hydraulic failure (Fig. 5). Values of  $A_r:A_l$  required to fit the data are given in Table 4.

TABLE A1. Soil parameters used in hydraulic failure analysis (see Appendix). Standard deviations are given for particle size percentages ( $n = 3$ ).

| Site                | Sand (%) | Silt (%) | Clay (%) | $K_s^*$ | $b$ | $\Psi_e$ | Soil type |
|---------------------|----------|----------|----------|---------|-----|----------|-----------|
| <i>vaseyana</i>     | 37 ± 9.6 | 33 ± 3.6 | 29 ± 6.4 | 8.9     | 8.3 | -2.4     | clay loam |
| <i>wyomingensis</i> | 53 ± 3.0 | 27 ± 4.7 | 20 ± 6.1 | 20.6    | 6.3 | -1.7     | loam      |

Notes:  $K_s^*$ , saturated soil conductivity ( $\text{mol}\cdot\text{s}^{-1}\cdot\text{MPa}^{-1}\cdot\text{m}^{-1}$ );  $b$ , dimensionless soil texture parameter (Eq. A.2) from Campbell (1985),  $\Psi_e$ , air entry pressure (kPa, Eq. A.2). Values for  $K_s^*$ ,  $b$ , and  $\Psi_e$  were calculated from texture data based on Campbell (1985).